Macromolecules

ARTICLE

pubs.acs.org/Macromolecules

Atomistic Structure Generation and Gas Adsorption Simulations of Microporous Polymer Networks

Lauren J. Abbott and Coray M. Colina*

Department of Materials Science and Engineering, The Pennsylvania State University, University Park, Pennsylvania 16802, United States

ABSTRACT: A new general procedure for generating structures for atomistic simulations of network polymers is presented. In the presented algorithm, cross-linking and chain formation occur in cycles along with equilibrations to "polymerize" microporous polymer networks. The procedure was validated by application to a hyper-cross-linked polymer, poly(dichloroxylene), but can be applied to other polymer networks as well. The simulated samples were characterized by cross-linking degrees and porosity measurements, and their adsorption behavior was simulated by grand canonical Monte Carlo (GCMC) simulations. Two important factors in generating samples with significant microporosity were determined: (a) the degree of cross-linking and (b) the concentration of the system during cross-linking. The effects of these two factors were examined and compared to similarly observed experimental trends. The methodology presented here is thus a promising technique for designing not only hyper-cross-linked polymers but also new amorphous, microporous polymers in general.

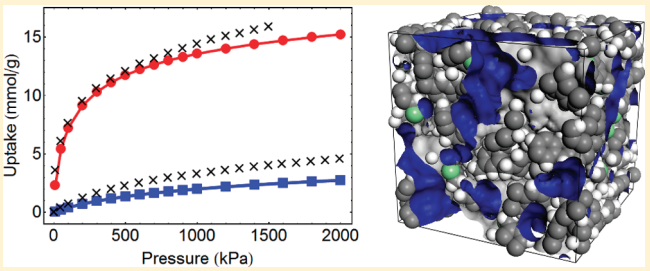

1. INTRODUCTION

Microporous materials, which have pores smaller than 2 nm, are of increasing importance for a number of applications, including separations, gas storage, and heterogeneous catalysis.[1] The porosity of a material, and specifically the pore size distribution, has a significant impact on its adsorptive properties. Many microporous materials of interest are crystalline, such as zeolites, metal−organic frameworks (MOFs),[2] and covalent organic frameworks (COFs)[3] because their pore structures are well understood and can therefore be tailored for specific applications. Amorphous materials have also proved useful for these types of applications, for example activated carbons,[4,5] polymers of intrinsic microporosity (PIMs),[6] and hyper-cross-linked polymers (HCPs).[7] However, the unordered nature and complex pore structures make these materials more difficult to characterize. Experimental characterization of porous materials is most often achieved through the use of gas adsorption, from which surface areas and pore size distributions can be derived. These characterization techniques, however, are based on many assumptions that compromise their certainty for amorphous, microporous materials. An alternative and complementary route for characterizing these materials is thus provided by molecular simulations, since surface areas and pore size distributions, for example, can be obtained directly by geometrical calculations.

Hyper-cross-linked polymers are a class of amorphous, microporous materials that possess permanent porosity due to their networked structure. There are mainly two synthesis routes for preparing HCPs. The first involves hyper-cross-linking polymer chains in solvent, resulting in the formation of pores.[8−10] An increased amount of free volume exists in the system while solvated, so when cross-linked the chains are locked in this expanded state in a way that pores remain when the solvent is removed. The second route is a polymerization of a system of monomers that allows for simultaneous formation of polymer chains and cross-links.[11,12]

Modeling HCPs and other amorphous networks is a nontrivial task due to their amorphous nature and the complexity of the networked structure. Computational approaches presented in the literature[11,13−19] often mimic one of the above synthesis routes for generating models of network polymers. Methods that mimic post-hyper-cross-linking of polymer chains create a simulation box packed with polymer chains, which are then cross-linked.[11,13] Alternatively, proposed methods also follow the synthesis route of simultaneous growth of chains and cross-links.[14−19] These schemes start with a simulation box packed with monomers, which are then cross-linked based on a predetermined set of rules. The system is "polymerized" by continuously cross-linking the monomers until a network results, with the formation of cross-links determined based on the proximity of monomers from one another.

When constructing HCPs starting from a system of monomers, the repulsive forces between monomers prevent them from packing too closely, so any cross-link formed will inevitably be longer than the equilibrium bond lengths. Energy minimizations and molecular dynamics (MD) simulations can be performed between the formations of cross-links to relax these bonds to reasonable lengths. However, if the bond lengths are too large, the strain induced on the system may not be relaxed adequately.

Received: February 9, 2011
Revised: April 14, 2011
Published: May 04, 2011

A cutoff distance criterion is usually applied to prevent this from happening. For example, Yarovsky and Evans[14] reported a 6 Å cutoff for epoxy resins, while Doherty et al.[15] used a cutoff in the range 4−6 Å for their poly(methacrylate) networks. It has also been shown[17] that performing an equilibration after every cross-link formation helps relieve the strain imposed on the system. However, this process can be computationally demanding, especially for larger systems. To lower computational costs, other work has examined performing more than one cross-link in each cycle. Varshney et al.[16] analyzed a dynamic cross-linking approach that cross-links all reactive pairs within a predefined cutoff range at once, within each cycle. They concluded that this procedure produced a well-relaxed system in a fraction of the iterations. This approach, however, requires a balance between introducing strain into the system and reducing computational cost.

This work aims at providing a detailed study of a computational approach for generating structures of HCPs and other network polymers, which cross-links a system of monomers. The procedure, inspired by those presented above, places significant importance on two main factors: (a) the degree of cross-linking and (b) the concentration of the system during cross-linking. The advantages of the proposed methodology are demonstrated through its application to poly(dichloroxylene), a HCP prepared by a step-growth polycondensation of dichloroxylene (DCX).[9,11] This system was chosen because of the relatively small size and simplicity of the monomer, as well as the experimental and computational studies available in the literature,[11,13,20] which allow for comparison to structural properties and adsorption behavior.

2. SIMULATION METHODS

2.1. Structure Generation Procedure. This work presents a computational procedure for generating initial structures of amorphous, network polymers for use in further simulations. The procedure was designed to mimic, to some extent, one synthesis route for HCPs, where the chains and cross-links are formed simultaneously. HCPs prepared by post-cross-linking of polymer chains could also be generated, however, with few alterations. In this work, cross-linking is performed initially at low densities to allow pores to form, after which the system is relaxed and compressed to achieve realistic, experimental-like densities.

By defining a monomer unit, its reactive atoms, and cross-linking sites, the proposed structure generation procedure can be applied to achieve a simulated structure with any degree of cross-linking. The presented algorithm is composed of three steps: (a) initial packing of the simulation box, (b) a cross-linking procedure, and (c) a compression and relaxation protocol.

A. Initial Packing of the Simulation Box. Monomers are packed into a simulation box under periodic boundary conditions using a Monte Carlo-like technique. By this approach, rigid monomers are placed into the box in a stepwise fashion, where insertions associated with lower energies are more probable. Once a desired density of monomers is obtained, an energy minimization is performed to reduce the net forces on the atoms. The resulting structure is in a more favorable state and provides a starting configuration for the following steps.

B. Cross-Linking Procedure. A cross-linking procedure has been designed to generate a networked structure from the packed simulation box created in the first step. It is controlled by two factors: (a) the degree of crosslinking (DOC) and (b) the density of the system during cross-linking. In the proposed algorithm, described in Scheme 1, bonds are formed in cycles, separated by short equilibrations, until a predefined degree of cross-linking is reached. As applied to poly(DCX), the algorithm is as follows:

Scheme 1. Cross-Linking Procedure Flowchart

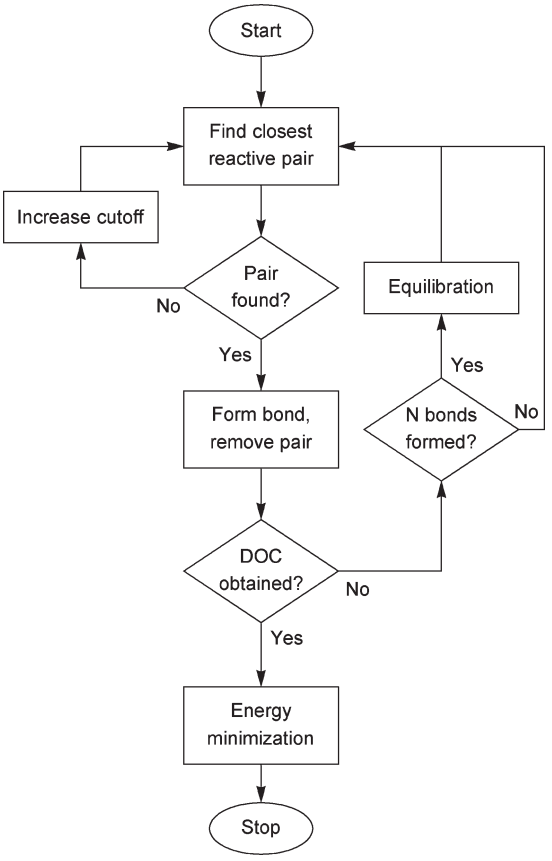

Step 1. The closest reactive pairs within the specified cutoff range are identified, which for DCX includes a chlorine atom and an aromatic hydrogen atom (Figure 1a). If no pairs exist in this range, the maximum cutoff is gradually increased until one is found. Since the distance between reactive pairs tends to increase at higher cross-linking degrees, a maximum possible cross-linking cutoff (6 Å in this work) is imposed to prevent the formation of unreasonably long bond lengths in the system.

Step 2. A bond is formed between the cross-linking sites associated with the closest reactive pair identified in step 1. In the case of DCX, this occurs according to Friedel−Crafts alkylation, which is simulated by removing the hydrogen and chlorine atoms and forming a bond between their associated carbon atoms (Figure 1b).

Step 3. Steps 1 and 2 are repeated *N* times. A short equilibration is then performed to relax the system (Figure 1c). This composes one cross-linking cycle. An equilibration step consists of, at the very least, an energy minimization but may also include a short MD step (NVT or NPT). NVT steps provide a more thorough relaxation, while NPT steps allow for a gradual compression of the structure throughout the procedure.

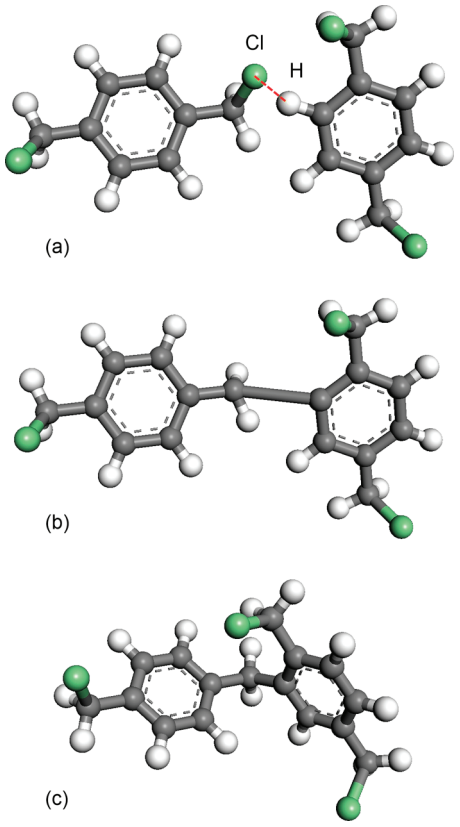

Figure 1. Example snapshots of a bond formation during the cross-linking procedure. (a) The closest reactive pair is identified, which includes a chlorine atom and an aromatic hydrogen atom in dichloroxylene. (b) A bond is formed between the cross-linking sites (the associated carbon atoms) and then the reactive atoms are removed. (c) An equilibration is performed. Note: carbon atoms are gray, hydrogen atoms are white, and chlorine atoms are green.

Step 4. Cross-linking cycles (steps 1−3) are executed until the target degree of cross-linking is reached. At completion, a final energy minimization is performed to ensure that a favorable final structure is obtained before relaxing and compressing the structure. Final structures are checked after completion to ensure that no ring spearing occurred during bond formations. Note that these checks alternatively could be implemented into the algorithm before a bond is made instead of at the completion of the cross-linking procedure.

C. Compression and Relaxation. The final step of the structure generation procedure is a 21-step compression and slow-decompression protocol, as proposed by Larsen et al.[21] The MD steps alternate between NVT and NPT simulations at various temperatures and pressures to represent annealings, coolings, compressions, and decompressions. The protocol allows the system to explore different configurations, while simultaneously compressing it to densities consistent with experimental values, and results in a well-relaxed, realistic final structure. The incorporation of a slow decompression was shown to produce structures with consistent final densities and was independent of the maximum pressure used.

The 21-step compression protocol consists of seven cycles, each cycle consisting of (i) an NVT step at 600 K, (ii) an NVT step at 300 K, and (iii) an NPT step at 300 K. The pressure at each cycle is increased stepwise in the first three cycles to the maximum pressure, which was 1.0 GPa in this work, and then slowly decompressed over the final four cycles to a final pressure of 0.0001 GPa (1 bar).[21] The total length of the compression protocol performed in this work was 1.76 ns, which includes 1 ns at the final NPT step at 0.0001 GPa to allow the system to fully equilibrate, such that the system remained at a constant average density.

2.2. Simulation Models. Using the presented structure generation procedure, a variety of atomistic simulated samples of poly(DCX) were created to both validate the procedure and study the effects of several parameters on the final structures (as discussed in the next section). Although hyper-cross-linked polymers have been observed to obtain mesopores, it has been suggested by Cooper and co-workers[11] that these larger pores would not contribute significantly to the adsorption behavior of the materials, which is a primary interest of this work. Hence, since in this work it is important to maintain full atomistic detail to most accurately represent the porosity of the samples, and the inclusion of mesopores would require significantly larger simulation samples, the study of the mesoporosity of these materials are outside the scope of the present work.

Two sets of simulations were performed with poly(DCX) to study the effect of the cross-linking parameters on the resulting structure and porosity. Larger simulation boxes (∼48 Å box length, 580 monomers) were generated with varying degrees of cross-linking. Additionally, smaller simulation boxes (∼32 Å box length, 176 monomers) were also created to study the effects of other cross-linking parameters, such as the system concentration and type of equilibration between cycles. Comparison of the smaller and larger boxes showed no major differences in structural or adsorptive properties, and thus the use of the smaller boxes significantly reduced the computational time of the simulations.

All atomistic procedures and simulations were carried out using the Materials Studio 5.0 software package[22] with the polymer consistent force field (pcff).[23] Molecular dynamics simulations were performed with the Forcite module, using a time step of 1 fs, the Nosé-Hoover thermostat with a Q ratio of 0.01, and the Andersen barostat with a time constant of 1 ps. Energy minimizations were also performed in the Forcite module, with a cascade of steepest descents, Newton−Raphson, and quasi-Newton methods. The Amorphous Cell module was used to pack the initial simulation boxes during the structure generation procedure.

Adsorption isotherms were calculated by grand canonical Monte Carlo (GCMC) simulations in the Sorption module. At each pressure, $(1-2) \times 10^7$ MC steps were performed, with a combination of translation, rotation, insertion, and deletion steps, to obtain equilibrium. All-atom models of hydrogen and methane were used. Nonbonded van der Waals interactions were estimated using a 9−6 Lennard-Jones potential, and Coulombic interactions were calculated using Ewald sums.

3. RESULTS AND DISCUSSION

3.1. Validation of Procedure. The proposed algorithm has been designed to mimic the synthesis methods of hyper-cross-linked polymers such that the cross-linking procedure is controlled by (a) the degree of cross-linking and (b) the concentration of the system during cross-linking. In this way, the structure generation procedure, as proposed, constrains only the degree of

cross-linking and the simulated density of the system during cross-linking. Hence, their properties, including porosity and adsorption behavior, can be considered predictive. In order to validate the algorithm and ensure that the simulated structures achieved are realistic, the simulated samples should be characterized and compared to experimental data.

The experimental characterization of microporous materials, such as HCPs, is not direct. For example, many structural properties are approximated indirectly from adsorption isotherms, such as surface areas, pore volumes, and pore size distributions. In molecular simulations, these properties can be measured directly by geometric methods. For this reason, comparison of properties calculated in simulations and experiments is not straightforward, and therefore the best way to validate the simulated structures is to compare an array of data. Properties compared in this work include cross-linking percentages, densities, surface areas, pore volumes, pore size distributions, and adsorption isotherms.

An important characteristic of HCPs is the degree of cross-linking, as this determines the rigidity of the network. The cross-linking degree can be estimated experimentally in poly(DCX) by elemental analysis, specifically the chlorine weight percentage.[11] Since the system loses a chlorine atom with each cross-link formed, the weight percent of chlorine in the system can be a good indicator of the cross-linking degree achieved in a sample. Experimental values of chlorine weight percent in poly(DCX) have been reported to be ~5 wt %.[11] In simulations, the number of cross-links formed in a sample can be counted directly, and so the degree of cross-linking can be exactly measured. One hundred percent cross-linking in poly(DCX) is defined in this work such that each aromatic ring has, on average, three bonds; that is, each monomer unit in a polymer chain participates in one cross-link.[7] Using this definition, simulated samples were generated with a cross-linking percentage of 122% to correspond to 5 wt % chlorine.

The resulting structures were then characterized in terms of their porosity, with surface areas, pore volumes, and pore size distributions. These properties are determined geometrically in simulations by defining surfaces in relation to the framework atoms. The simplest surface can be defined as the van der Waals surface, which is the surface traced out by the van der Waal radii of the framework atoms. However, this overestimates the amount of volume or surface that is actually accessible to a molecule. Therefore, Connolly and accessible surfaces are defined by "rolling" a probe molecule across the surface of the framework atoms, such that there is no overlap with any of the framework atoms. The Connolly surface is taken from the edge of the probe molecule, while the accessible surface is taken from the center. In this way, pores that are smaller than the probe size are not included in the surface and volume calculations.

Previous work by Düren et al.[24] with MOFs reported that accessible surface areas are more appropriate for characterizing porous solids than Connolly surface areas, as they more accurately describe the amount of surface accessible to a probe molecule. For pore volumes and pore size distributions, however, the Connolly surface is the correct choice. This is because the Connolly surface takes into account the volume accessible to any part of the probe and more accurately represents the physical size of the pores.[4] Thus, in this work surface areas were calculated from the accessible surface, while pore volumes and pore size distributions were obtained with Connolly surfaces. It should be noted that, by the nature of the definition of these surfaces, the measured surface areas and pore volumes depend on the size of the probe molecule. Since experimentally they are calculated from nitrogen sorption isotherms, a probe diameter of 3.681 Å[24] was used in this work, equal to the kinetic diameter of a nitrogen molecule.

For the simulated structures of poly(DCX), the average surface area and pore volume of five independent simulation boxes are given in Table 1. The average simulated surface area of 671 m^2/g and pore volume of 0.32 cm^3/g are significantly smaller than the reported[11] experimental BET surface area (1370 m^2/g) and pore volume (0.494 cm^3/g). However, it has been noted before that BET surface areas are overestimated in systems with small micropores,[4,25] such as poly(DCX), so it is not surprising that a smaller value is seen in simulations. Also, it must be noted that BET surface areas are calculated based on a number of assumptions, such as a slit-pore geometry, and cannot be considered a direct comparison to geometrically calculated surface areas in simulations.

The determination of densities in experiment and simulation are inherently different. Experimentally, densities are calculated from the skeletal volume of the sample, where the volume of the sample is determined by the volume inaccessible to gas molecules. In this way, the volume contributed by the pores is excluded. In simulations, however, the density is calculated using the total volume of the simulation box. Skeletal densities can be calculated from simulated densities by subtracting the pore volume per unit mass. This is given by the relationship $1/\rho_{skel} = 1/\rho_{sim} - v_{pore}/m$, where ρ_{skel} is the skeletal density, ρ_{sim} is the simulation density (total mass over total volume), v_{pore} is the pore volume, and m is the total mass of the system. Using this conversion, the skeletal densities calculated for the simulated structures are more directly comparable to experimentally reported values.

In addition to measuring the porosity of the samples, GCMC simulations can be performed to estimate the adsorption of gases in the adsorbent. In Figure 2, adsorption isotherms for the simulated samples summarized in Table 1 are shown together with experimental data of Cooper and co-workers.[11,20] The simulated hydrogen and methane isotherms were calculated at 77 and 300 K, respectively, up to 2000 kPa. Comparison with the experimental results shows excellent agreement in shape and magnitude. The isotherms display enhanced loading at low pressures followed by leveling off to a plateau at high pressures, which is characteristic of microporous materials. It is important to note that no scaling factors have been applied to the isotherms calculated in this work. Previous computational work with poly(DCX) reported by Cooper and co-workers[11,13,20] applied large scaling factors (0.36−0.45) to obtain quantitative agreement with experimental data. In this work, however, the isotherms are presented as predicted by the GCMC simulations.

While our simulated hydrogen adsorption isotherm is quantitatively consistent with experimental results, there is an underprediction for the simulated methane adsorption. This might be related with the larger size of the methane molecule (kinetic diameter of 3.8 Å) compared to a hydrogen molecule (kinetic diameter of 2.89 Å), such that fewer pores are accessible to methane. Calculated surface areas using these probe diameters for methane and hydrogen yield 618 and 1123 m^2/g, and corresponding pore volumes were found to be 0.315 and 0.375 cm^3/g. These values confirm that the accessible surface area and pore volume is significantly smaller for the methane molecules, suggesting that a number of pores exist in the size range 2.9−3.8 Å.

Table 1. Structural Properties of Simulated Samples of Poly(dichloroxylene)

	box size (Å)	cross-linking (%)	chlorine (wt %)	skeletal density (g/cm^3)	surface area (m^2/g)	pore volume (cm^3/g)
simulation[a]	32.4 ± 0.3	122	5.40	1.33 ± 0.01	671 ± 100	0.32 ± 0.03
experiment[11]			5.24[b]	1.280[c]	1370[d]	0.494[e]

[a] In this work, average values and standard deviations are reported for five independent simulated samples. [b] Chlorine wt % determined from elemental analysis. [c] Skeletal density measured by helium pycnometry. [d] BET surface area calculated from N_2 isotherm at 77.3 K. [e] Micropore volume calculated from N_2 isotherm at 77.3 K.

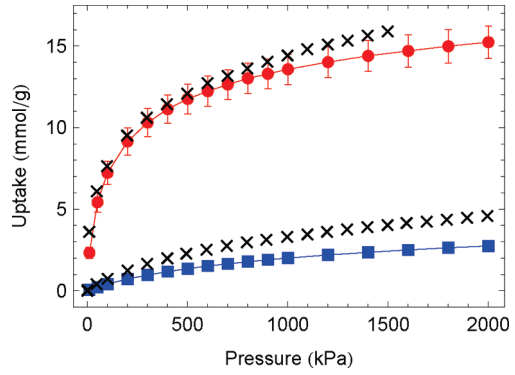

Figure 2. Hydrogen (●) and methane (■) adsorption isotherms calculated at 77 and 300 K, respectively, as compared to experimental isotherms[11,20] (×). Simulated isotherms are plotted as the average of five independent structures, with error bars given by the standard deviation. Note that the methane error bars are smaller than the symbols shown.

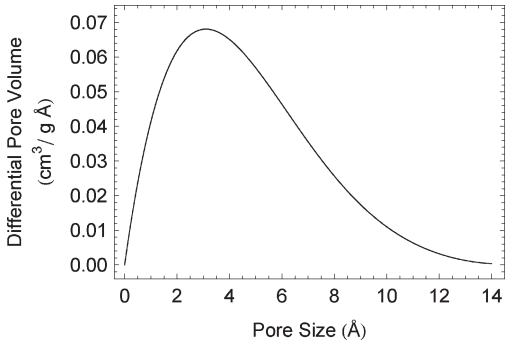

Figure 3. Average pore size distribution for simulated samples of poly(dichloroxylene). A large number of pores in the system are 1−5 Å, with a peak near 3 Å, and a tail extending to larger pore sizes up to 14 Å.

The average pore size distribution of the simulated samples, shown in Figure 3, provides further support for these statements. The samples show a peak near 3 Å, with a large number of pores in the range 3−4 Å. Pores of this size would be too small for methane molecules, but large enough for hydrogen molecules, accounting for the large differences in accessible volume and adsorption for the two. With a pore size distribution shifted slightly to larger pore sizes, it would be expected that better agreement would be obtained for the simulated methane isotherms. Additionally, a shift in the pore size distribution to larger pores would also result in an increased surface area and pore volume, which then would be more consistent with experimental values, as given in Table 1. Nevertheless, the predictive results presented in Table 1 and Figure 2 are encouraging.

As mentioned before, the simulated data presented in this section were averaged over five independent boxes to provide good statistics. The difficulty in simulating amorphous materials is in producing samples with consistent results. The reproducibility of the structure generation procedure was seen to significantly improve when the equilibration steps used in the cross-linking procedure contained a short MD step. NVT and NPT MD steps were found to have a positive effect on the relaxation of the system between cross-linking cycles, despite the modest increased computational time. When no MD steps were performed, the lengths of bonds formed during the cross-linking procedure tended to become larger at higher degrees of cross-linking. Performing short MD steps, however, significantly reduced the bond formation lengths and thus the strain induced on the system during cross-linking.

In the simulated samples reported in this section, a very short NPT or NVT MD step was performed during each equilibration. The MD steps, although short, provided enough time for a slight relaxation of the system during the cross-linking procedure and allowed the bond lengths formed to be of more realistic lengths than if no MD step was performed. The bond length distributions for one of the structures reported in this section, as compared to a sample generated with no MD step during equilibration, is shown in Figure 4. Although the bond lengths on average are still larger than the equilibrium bond length, the bond length distribution is much narrower when MD was performed.

3.2. Degree of Cross-Linking. A unique characteristic of HCPs is permanent porosity. This is possible due to the high degree of cross-linking, which allows for the formation of a rigid, porous network. At lower cross-linking degrees, HCPs are essentially nonporous, as the polymer chains are more mobile and able to pack more closely, preventing pores from forming. For this reason, the degree of cross-linking is one of the most important factors in creating a HCP with significant microporosity. To study the effect of the degree of cross-linking on the porosity and adsorption behavior, simulated structures were constructed with 66, 90, 122, and 133% cross-linking.

The effect of the cross-linking degree on the structure is clearly evident by the snapshots of simulated samples shown in Figure 5, which display the pore volumes as defined by the Connolly surface for cross-linking degrees of 66, 90, and 122%. Only the structure with 122% cross-linking has high free volume and pores of significant sizes. This is quantitatively supported by the characterization data presented in Table 2. In increasing the cross-linking from 90 to 122%, a significant rise can be seen in the surface area (25 to 683 m^2/g) and pore volume (0.065 to 0.318 cm^3/g). In both cases, the values are a magnitude of order larger. Samples cross-linked to 133% did not have significantly different properties than those with 122% cross-linking.

Larger simulation boxes were created in this section, with box sizes around 48 Å. In comparing the results of the larger boxes cross-linked to 122% with the smaller boxes presented in the

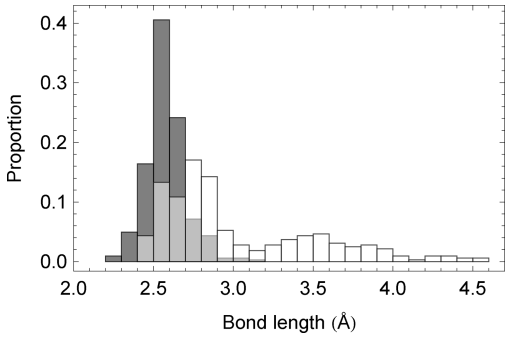

Figure 4. Histograms charting the distributions of bond lengths formed during the cross-linking procedure when the equilibration consists of only an energy minimization (white) or both an energy minimization and MD step (gray). The distribution is much narrower when MD is performed during the equilibration, suggesting that the system remains more relaxed than if no MD is performed. Note that the overlap between the two histograms is shown in a lighter gray.

previous section (in Table 1), no significant differences were observed in the properties of the samples. The larger box's surface area of 683 m^2/g and pore volume of 0.318 cm^3/g are in agreement with that of the smaller boxes, 671 m^2/g and 0.32 cm^3/g, respectively. Therefore, a similar comparison can be made between the larger simulated box and experimental data (presented in Table 1), as was done in the previous section with the smaller boxes.

In addition to structural properties, the adsorptive performance of the simulated samples highlights the effect of the degree of cross-linking on the generated structure. Hydrogen and methane adsorption isotherms at 77 and 300 K, respectively, calculated up to 1000 kPa using GCMC simulations, are shown in Figure 6. In both cases, the uptake is significantly lower with lower cross-linking degrees. For hydrogen, the uptake at 1000 kPa for the 122% cross-linking sample, about 13.5 mmol/g, was found to be more than 3 times larger than that in the 90% samples, which was about 4 mmol/g. The difference for methane is even higher, increasing from 0.26 to 2.06 mmol/g from the 90 to 122% cross-linking samples. This again reinforces the conclusion that the microporosity of a sample increases considerably with the degree of cross-linking.

As is evidence by characterization data, such as surface area, pore volume, and gas uptake, a significant increase in microporosity is seen in simulated samples with higher cross-linking degrees. This trend has also been observed experimentally.[7,11,12] Furthermore, the data suggest that the simulated structures of poly(DCX) with 122% cross-linking are most representative of the experimentally synthesized samples. It is important to recall that this cross-linking degree was not chosen because it most closely matched characterization data, but instead was determined by estimating experimental cross-linking degrees using the measured chlorine wt % by elemental analysis. As such, the characterization data can be considered predictive, based on the degree of cross-linking obtained.

It should be mentioned that the chlorine wt % provided by elemental analysis is only an approximation of the degree of cross-linking and not a direct measurement. Extra chlorine atoms could remain in the system trapped in voids, released either during cross-linking or from residual solvent, which would therefore affect the chlorine wt % measured experimentally. This is not the case in the simulated samples. It is therefore possible

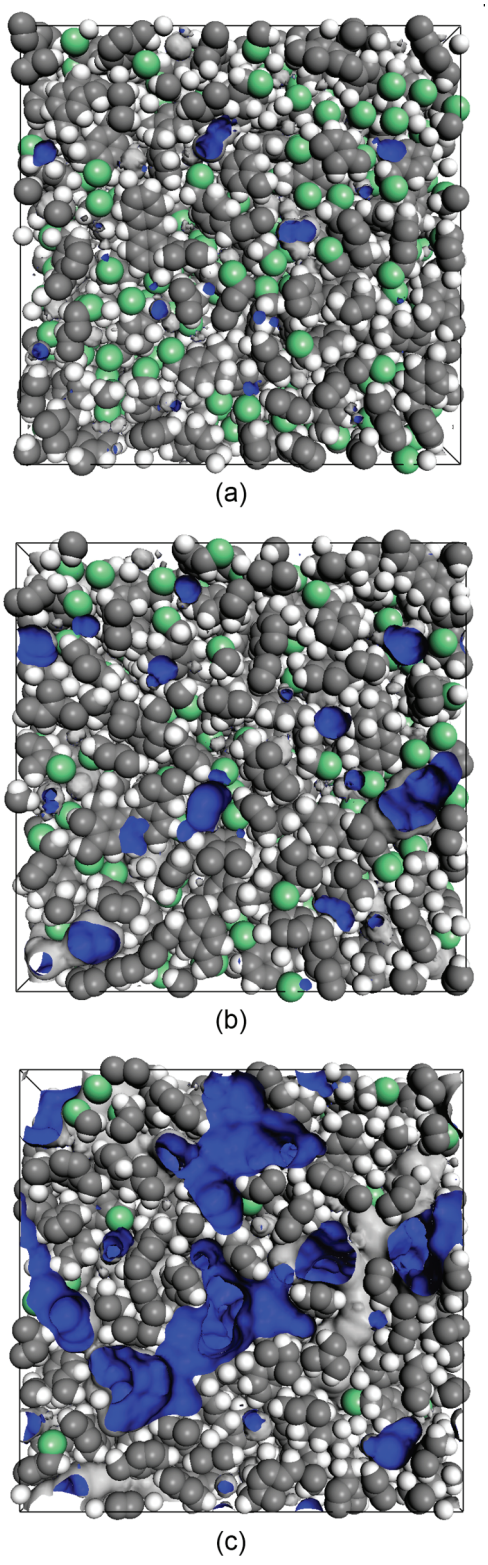

Figure 5. Snapshots of simulation boxes with (a) 66, (b) 90, and (c) 122% cross-linking. The Connolly surfaces are highlighted in blue, which represent the pore volume within the structures. It is clear from the sizes of the pores that the sample with 122% cross-linking is microporous, while the samples with 66 and 90% cross-linking can be considered nonporous. As in Figure 1, carbon atoms are gray, hydrogen atoms are white, and chlorine atoms are green.

Table 2. Structural Properties of Simulated Samples of Poly(dichloroxylene) with Varying Degrees of Cross-Linking

box size (Å)	cross-linking (%)	chlorine (wt %)	skeletal density (g/cm^3)	surface area (m^2/g)	pore volume (cm^3/g)
48.08	66	25.58	1.239	1	0.026
47.22	90	18.37	1.244	25	0.065
48.24	122	5.53	1.319	683	0.318

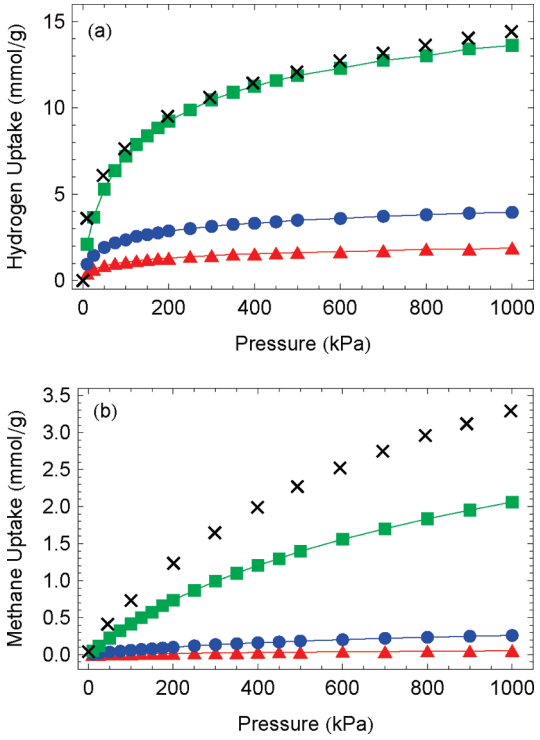

Figure 6. (a) Hydrogen and (b) methane adsorption isotherms calculated at 77 and 300 K, respectively, for simulated structures with 66% (▲), 90% (●), and 122% (■) cross-linking, as compared with experimental isotherms[11,20] (×). Results show a significant increase in uptake with higher degrees of cross-linking.

that a higher degree of cross-linking is achieved experimentally than has been estimated here. However, simulated structures with 0 wt % chlorine (133% cross-linking) were generated (not shown), and no significant differences in structure from samples with 5 wt % chlorine (122% cross-linking) were observed.

The results presented in this section suggest that porosity does not increase linearly with cross-linking, but instead requires a minimum cross-linking degree to introduce permanent porosity, after which little structural changes occur. This can be observed by the changes in porosity of the simulated structure with increasing cross-linking degrees of 66, 90, 122, and 133%. Only a small increase in porosity is observed upon increasing the degree of cross-linking from 66 to 90%, where the samples could still be considered nonporous. However, a dramatic increase in porosity is obtained when extended to 122% cross-linking. Then, almost no significant further change in porosity resulted upon reaching 133% cross-linking. Similar trends can be seen for experimental studies of hyper-cross-linked polymers cross-linked to varying degrees, where a dramatic increase in surface area is

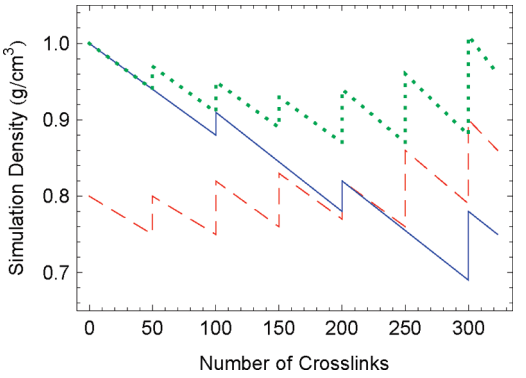

Figure 7. Density of the system during the cross-linking procedure as a function of the number of the cross-links formed, using schemes 1 (– –), 2 (—), and 3 (· · ·), with parameters as defined in Table 3. The steady decreases in the density occur when cross-links are formed and the reactive atoms are removed. Each step in the density corresponds to an equilibration during the cross-linking procedure for which an NPT compression is performed.

observed followed by a leveling off at higher cross-linking degrees.[7,11,12]

3.3. System Concentration. In addition to the degree of cross-linking, the concentration of the system during cross-linking was found to have a significant impact on the microporosity of the simulated samples. HCPs derive their porosity from the expanded solvated state in which they are cross-linked. When cross-links are formed throughout the material, the structure is locked in a configuration favoring this expanded state, such that pores are preserved when the solvent is removed. Therefore, an expanded state during cross-linking is crucial to formation of microporous structures. This effect has been observed experimentally[7,11] by varying the concentration of the monomers or polymers in solvent during cross-linking. In doing this, samples cross-linked at higher concentrations had lower porosity, as displayed by the obtained surface areas and pore volumes.

During the simulated structure generation procedure described in section 2.1, a "solvated state" is mimicked by maintaining the system at low densities. This is determined by, first, the initial packing density of the monomers and subsequently the density of the system during cross-linking. If the density is too high, cross-linking locks the system in a dense state, restricting the formation of pores. However, if the density is too low, bond lengths formed near the end of the procedure can be large, potentially causing unrealistic configurations within the structure and high levels of strain.

Since the density of the system drops with the formation of each cross-link, as atoms are removed from the system, further steps must be taken to ensure that the density of the system remains within a desired range. During the cross-linking procedure, the density can be continuously adjusted by including NPT MD simulations during the equilibration step between cross-linking cycles. Controlling the concentration of the simulation samples, however, requires a delicate balance of the frequency and length of the NPT steps. If performed too often or for too long, the system will quickly be compressed to a high density and prevent the formation of pores. To accomplish this, NPT MD steps are not performed between every cycle of the cross-linking procedure, but every M cycles instead. Therefore, a short MD step (NPT or NVT) is performed during every equilibration.

Table 3. Structural Properties of Simulated Samples of Poly(dichloroxylene) with Different Equilibration Schemes To Adjust Sample Densities during Cross-Linking[a]

scheme	box size (Å)	monomer concn (g/cm^3)	no. of bonds between NPT steps	length of MD steps (ps)	skeletal density (g/cm^3)	surface area (m^2/g)	pore volume (cm^3/g)
1	32.1 ± 0.3	0.8	50	5	1.327 ± 0.009	600 ± 100	0.29 ± 0.03
2	32.4 ± 0.3	1.0	100	1	1.33 ± 0.01	671 ± 100	0.32 ± 0.03
3	31.1 ± 0.2	1.0	50	5	1.315 ± 0.009	274 ± 30	0.20 ± 0.02

[a] Average values and standard deviations are reported for five independent simulated samples. These schemes correspond to those in Figures 7 and 8, schemes 1 (– –), 2 (—), and 3 (···). The results for scheme 2 are also presented in Table 1.

These alternate between NVT steps, which maintain the box size, and NPT steps every M cycles, which allow for a slight compression.

Three different schemes were developed varying the density during the cross-linking procedure to study its effect on the final structure and porosity of the samples. The parameters controlling the density of the system during cross-linking include (a) the initial packing density of the monomers, (b) the length of the NVT/NPT MD step during the equilibration, and (c) how often the MD step is NPT instead of NVT. The frequency of the NVT step thus can be measured as occurring every M cycles, or every $N \times M$ bonds, if N bonds are performed in each cycle. The three schemes are best described by plotting the density of the systems during the cross-linking procedure as a function of the number of cross-links formed, as shown in Figure 7. The average simulation densities during the cross-linking procedure for schemes 1, 2, and 3 are 0.80, 0.83, and 0.94 g/cm^3, respectively. These densities are representative of the expanded state during cross-linking and are different than the final densities achieved after the compression scheme is performed (final skeletal densities are given in Table 3).

The parameters of the three schemes and average properties for five independent samples generated using these schemes are presented in Table 3. After the compression scheme was performed, the final skeletal densities of the boxes are similar, 1.31−1.33 g/cm^3, with variations arising from the different porosities obtained using the three schemes. From the surface areas and pore volumes, it can be concluded that schemes 1 and 2 result in samples that are significantly more porous. For example, their surface areas are both at least 600 m^2/g, while scheme 3 results in samples with surface areas averaging only 274 m^2/g. Through comparison of the three schemes, the resulting porosities of the samples show trends similar to those observed experimentally,[7,11] where higher concentrations during cross-linking prevent significant porosity from forming.

The schemes were further examined by calculating the pore size distributions of the simulated samples, which are shown in Figure 8. The pore size distribution for samples generated with scheme 3 show a significantly smaller proportion of larger pores, with very few pores above 6−8 Å. The lower values of surface area and pore volume can be attributed to this distribution. Schemes 1 and 2, on the other hand, have a greater proportion of larger pores of sizes 8−14 Å. Although the range of pore sizes is similar, the distribution is slightly different. The plotted pore size distributions suggest that scheme 2 generates a more even distribution of pore sizes, whereas scheme 1 appears to result in a broader range of larger pores. In this work with poly(DCX), scheme 2 produced simulated structures most representative of experimental samples, as the values of surface area and pore volume are larger and most similar to experimental data. Thus,

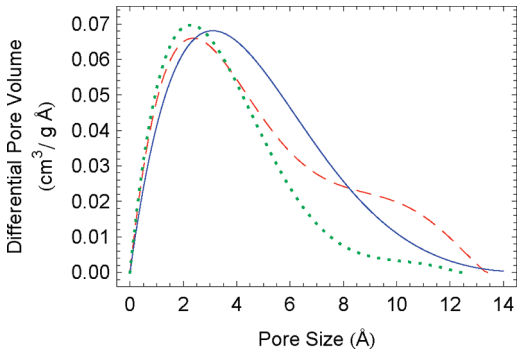

Figure 8. Average pore size distributions for sets of samples of poly(dichloroxylene), which maintain different concentrations during the cross-linking procedure, as described by schemes 1 (– –), 2 (—), and 3 (···) defined in Table 3. The pore size distribution for scheme 2 is also given in Figure 3. Note that the color scheme corresponds to the same sets as in Figure 7.

the results presented in section 3.1 use this scheme. However, if a higher proportion of larger pores is desired, it can be readily designed using scheme 1.

The analysis of equilibration schemes presented in this section has shown the importance of the system density during cross-linking. Porosity in HCPs is derived from the solvated state in which they are cross-linked, which is essential to forming micropores. During the cross-linking procedure, this expanded solvated state is reproduced by maintaining the system at a low density. As has been seen experimentally,[7,11] low porosity is obtained in HCPs if the concentration of the system is too high during cross-linking. Therefore, the density of the simulated structures during cross-linking, as determined by the initial packing density and the length and frequency of NPT MD compression steps, is an important factor in controlling the microporosity of the simulated samples generated using the presented algorithm. To control the porosity of simulated samples of HCPs, protocols can be designed as suggested by the three schemes presented in this work to generate structures with varying levels of porosity. For poly(DCX) and similar HCPs with high porosity and desirable adsorption properties, the proposed algorithm with scheme 2 should be used.

4. CONCLUSIONS

In this work, we have presented a new procedure for generating atomistic structures for simulating network polymers, where networks are formed by a cross-linking procedure that "polymerizes" a system of monomers in a stepwise fashion. Although general to polymer networks, the algorithm was validated for hypercross-linked polymers through application to poly(dichloroxylene).

Simulated structures were characterized in terms of their porosity and compared to experimental data. Because of the inherent differences in calculating properties experimentally and in simulations, such as resulting from indirect measurements and theoretical approximations, simulated samples were validated by comparison to a range of properties. Gas adsorption isotherms of hydrogen and methane were also predicted using grand canonical Monte Carlo (GCMC) simulations.

Further analysis of the cross-linking procedure determined two important factors for producing microporosity in hyper-cross-linked polymers: the degree of cross-linking and the density of the system during the cross-linking procedure. A low density during cross-linking was shown to be crucial for allowing pores to form within the network, while a high number of cross-links within the system was needed to lock the network in the expanded state. The detailed analysis of these effects on the simulated hyper-cross-linked polymer systems were seen to display similar trends in qualitative agreement with experimental results. Predicted isotherms showed quantitative agreement to experimental data, without scaling factors. The methodology presented here is thus a promising technique for designing not only hyper-cross-linked polymers but also new amorphous, microporous polymers in general.

AUTHOR INFORMATION

Corresponding Author
*E-mail: colina@matse.psu.edu.

ACKNOWLEDGMENT

The authors thank the National Science Foundation (DMR-0908781) for funding. High performance computational resources for this research were provided by the Materials Simulation Center and the Lion-HPC systems of Penn State Information Technology Services.

REFERENCES

(1) Schüth, F.; Sing, K. S. W.; Weitkamp, J. *Handbook of Porous Solids*; Wiley-VCH: Weinheim, Germany, 2002.
(2) Eddaoudi, M.; Kim, J.; Rosi, N.; Vodak, D.; Wachter, J.; O'Keeffe, M.; Yaghi, O. M. *Science* **2002**, *295*, 469–472.
(3) El-Kaderi, H. M.; Hunt, J. R.; Mendoza-Cortés, J. L.; Côté, A. P.; Taylor, R. E.; O'Keeffe, M.; Yaghi, O. M. *Science* **2007**, *316*, 268–272.
(4) Gelb, L. D.; Gubbins, K. E. *Langmuir* **1998**, *14*, 2097–2111.
(5) Gelb, L. D. *MRS Bull.* **2009**, *34*, 592–601.
(6) McKeown, N. B.; Budd, P. M. *Macromolecules* **2010**, *43*, 5163–5176.
(7) Tsyurupa, M. P.; Davankov, V. A. *React. Funct. Polym.* **2006**, *66*, 768–779.
(8) Germain, J.; Fréchet, J. M. J.; Svec, F. *J. Mater. Chem.* **2007**, *17*, 4989–4997.
(9) Tsyurupa, M. P.; Davankov, V. A. *React. Funct. Polym.* **2002**, *53*, 193–203.
(10) Pastukhov, A. V.; Tsyurupa, M. P.; Davankov, V. A. *J. Polym. Sci., Part B: Polym. Phys.* **1999**, *37*, 2324–2333.
(11) Wood, C. D.; Tan, B.; Trewin, A.; Niu, H.; Bradshaw, D.; Rosseinsky, M. J.; Khimyak, Y. Z.; Campbell, N. L.; Kirk, R.; Stöckel, E.; Cooper, A. I. *Chem. Mater.* **2007**, *19*, 2034–2048.
(12) Zeng, S.-Z.; Guo, L.; He, Q.; Chen, Y.; Jiang, P.; Shi, J. *Microporous Mesoporous Mater.* **2010**, *131*, 141–147.
(13) Trewin, A.; Willock, D. J.; Cooper, A. I. *J. Phys. Chem. C* **2008**, *112*, 20549–20559.
(14) Yarovsky, I.; Evans, E. *Polymer* **2002**, *43*, 963–969.
(15) Doherty, D. C.; Holmes, B. N.; Leung, P.; Ross, R. B. *Comput. Theor. Polym. Sci.* **1998**, *8*, 169–178.
(16) Varshney, V.; Patnaik, S. S.; Roy, A. K.; Farmer, B. L. *Macromolecules* **2008**, *41*, 6837–6842.
(17) Wu, C.; Xu, W. *Polymer* **2006**, *47*, 6004–6009.
(18) Lin, P.-H.; Khare, R. *Macromolecules* **2009**, *42*, 4319–4327.
(19) Komarov, P. V.; Yu-Tsung, C.; Shih-Ming, C.; Khalatur, P. G.; Reineker, P. *Macromolecules* **2007**, *40*, 8104–8113.
(20) Wood, C. D.; Tan, B.; Trewin, A.; Su, F.; Rosseinsky, M. J.; Bradshaw, D.; Sun, Y.; Zhou, L.; Cooper, A. I. *Adv. Mater.* **2008**, *20*, 1916–1921.
(21) Larsen, G. S.; Lin, P.; Hart, K. E.; Colina, C. M. *Macromolecules* **2011**, submitted.
(22) Accelrys Software Inc., Materials Studio, Release 5.0; Accelrys Software Inc., San Diego, 2009.
(23) Sun, H. *J. Comput. Chem.* **1994**, *15*, 752–768.
(24) Düren, T.; Millange, F.; Férey, G.; Walton, K. S.; Snurr, R. Q. *J. Phys. Chem. C* **2007**, *111*, 15350–15356.
(25) Roque-Malherbe, R. M. A. *Adsorption and Diffusion in Nanoporous Materials*; CRC Press: Boca Raton, FL, 2007.